Progress In Electromagnetics Research M, Vol. 32, 129–143, 2013

A SIMPLE TECHNIQUE FOR IMPROVING THE ANECHOIC PERFORMANCE OF A PYRAMIDAL ABSORBER

Muhammad N. Iqbal[1, *], Fareq Malek[2], Yeng S. Lee[1], Liyana Zahid[2], Muhammad I. Hussain[3], Mohd F. H. A. Malek[4], Nur F. M. Yusof[2], Norshafinash Saudin[2], and Noor A. A. Talib[2]

[1]School of Computer and Communication Engineering, Universiti Malaysia Perlis (UniMAP), Pauh Putra Campus, Arau, Perlis 02600, Malaysia

[2]School of Electrical System Engineering, Universiti Malaysia Perlis (UniMAP), Pauh Putra Campus, Arau, Perlis 02600, Malaysia

[3]School of Manufacturing Engineering, Universiti Malaysia Perlis (UniMAP), Pauh Putra Campus, Arau, Perlis 02600, Malaysia

[4]MISC Liaison LNG Liaison Office Japan, MISC Berhad, Yokohama, Japan

Abstract—In this paper, we propose a very simple technique that offers an extra degree of freedom to optimize the design of a tire dust-based absorber with reduced height. Cladding is a technique that is used to enhance the surface properties of a part, and it has been used in many applications for many years. In this technique, a clad layer is created on the core material, and the composition of the clad layer is adjusted to enhance the performance of the core material. We use a rice husk-clad layer to enhance the impedance matching characteristics of the low-loss, tire-dust core, microwave absorber. The overall design is a two-layer, geometrically-tapered, pyramidal structure composed of two lossy waste materials. Our main goal was to make the front surface less reflective (impedance matched), hence the material of the outer layer (clad) of the absorber was selected on the basis of the analysis of the dielectric properties of the candidate materials. Optimum thickness of the clad was obtained by using CST simulation software and found to be 12 mm, for which a reflectivity performance of less than −20 dB was

Received 16 June 2013, Accepted 30 July 2013, Scheduled 31 July 2013

* Corresponding author: Muhammad Nadeem Iqbal (mr.nadeemiqbal@gmail.com).

achieved in the frequency range of 4 to 20 GHz. The results were found to be better than those provided by an earlier design of the absorber, which was composed of a mixture of tire dust and rice husks.

1. INTRODUCTION

Anechoic chambers are used to evaluate the electromagnetic compatibility (EMC) of military and commercially-available, electronic equipment. Electronic equipment is tested in these anechoic chambers for their emission levels and susceptibility in accordance with different, internationally-recognized standards that are well known in the civil and military domains [1, 2]. Currently, the most widely used broadband anechoic absorbers are made out of carbon impregnated polyurethane (PU) foam in pyramidal, wedge, and in convoluted shapes [3]. Although frequency selective surfaces (FSS) have been studied [4, 5], to improve the low frequency performance of these absorbers however, ferrite tiles are still preferred.

Recently, rice husk waste [6–15] and rubber tire-dust waste [14–16] have been studied and identified as effective microwave absorbing materials for the fabrication of microwave absorbers in pyramidal and wedge shapes. Rice husks comprise 22% of a rice paddy, and this waste material contains about 35 to 44% carbon [17, 18], whereas tire dust contains about 29 to 31% carbon [19, 20]. In [14], Malek et al. studied mixtures of rice husks and tire dust for the limited frequency range of 7 to 13 GHz. However, the reflectivity performance was not comparable to that of the rice husk-based absorber because the loss factor of the tire dust was less than that of the rice husks. Cheng et al. [15] suggested a mixture of 70% rice husks and 30% tire dust to solve this issue. In this paper, we present a very simple solution to improve the performance of tire dust-based absorbers. It is a well-known fact that the first reflection is always at the outer surface (impedance boundary) of the absorber and that the dissipation phenomenon within the absorbing material takes place later. Minimum values of reflection and transmission coefficients are required to improve the anechoic performance of an absorber. In order to accomplish these requirements, we introduced a low permittivity, high-loss layer (clad) of rice husks on a pyramidal, tire-dust absorber. Although we used the same materials studied in [14, 15], we are proposing a simple and advantageous approach that provides additional degrees of freedom to optimize the absorber design.

2. THEORETICAL BACKGROUND

We modeled the absorber as a two-layer structure. The first layer was used as a cladding, and it had a thickness (t_1). The second layer had a thickness (t_2), where $t_1 < t_2$. The second layer was used as a core, and both layers had pyramidal shapes, as shown in Figure 1.

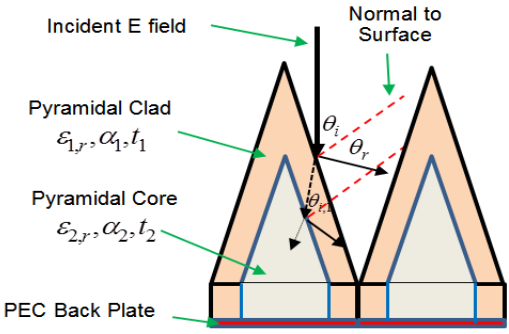

Figure 1. Illustration of the cladded, pyramidal microwave absorber and wave interaction at the interfaces.

The first layer had a relative complex permittivity of $\varepsilon_{1,r} = \varepsilon'_{1,r} - j\varepsilon''_{1,r}$, while the second layer had a relative complex permittivity of $\varepsilon_{2,r} = \varepsilon'_{2,r} - j\varepsilon''_{2,r}$. Both layers had the same relative complex permeability, i.e., $\mu_{1,r} = \mu_{2,r} = 1 + j0$ and $\varepsilon_{1,r} \neq \varepsilon_{2,r}$. Based on these constitutive parameters, each layer had a distinct characteristic impedance and $Z_1 \neq Z_2$, where $Z_1 = \cos\theta_i / \sqrt{\varepsilon_{1,r} - \sin^2\theta_i}$ and $Z_2 = \cos\theta_{i,1} / \sqrt{\varepsilon_{2,r} - \sin^2\theta_{i,1}}$, whereas θ_i and $\theta_{i,1}$ are the wave incident angles from the normal at the air-clad and clad-core interfaces, respectively. Since $\varepsilon_{1,r} > \varepsilon_0$ and $\varepsilon_{1,r} \neq \varepsilon_{2,r}$, hence $Z_1 < Z_0$ and $Z_1 \neq Z_2$, consequently an impedance step exists at the air-clad interface and at the clad-core interface. In order to minimize the reflections in a broad frequency range at the interfaces, the general procedure is to gradually transform the impedance, i.e., $Z_2 < Z_1 < Z_0$. However, this does not ensure the absorption of the wave within the absorber unless it is lossy enough to restrict the transmission of the wave.

The loss-gradient technique is used in commercial, multi-layer absorbers to dissipate the wave energy gradually. In our design, we used $Z_2 < Z_1 < Z_0$ and $\alpha_1 > \alpha_2$, which were the attenuation constants of the clad layer and the core, respectively. The benefit of this approach is that most of the energy of the incident wave

is attenuated exponentially as it traverses the clad layer, and the condition $e^{-\alpha_1 t_1} < e^{-\alpha_2 t_2}$ for $t_1 = t_2$ is satisfied. Under this condition, a thinner clad will be enough to dissipate the incident energy, and a wave with weak amplitude will arrive at the clad-core interface. Since the core is less lossy than the clad and $\alpha_2 < \alpha_1$, the large thickness of the core ($t_2 > t_1$) will compensate for this lack of loss.

3. DIELECTRIC PROPERTIES AND WAVE PROPAGATION

Several methods currently are used at microwave frequencies to measure the complex permittivity based on the reflection and transmission of the signal, including the coaxial line, wave-guide, and free-space methods [21–24]. We preferred the broadband open-ended, coaxial-probe method, which provided simple, straightforward, and non-destructive measurements of complex permittivity. The open end of the probe was pressed against the flat surface of the sample, and the complex reflection coefficient was measured. Then, Agilent software was used to retrieve the real and imaginary parts of the complex permittivity from the measured reflection coefficient data.

3.1. Complex Permittivity and Loss Tangent Spectra

Figures 2(a) and (b) show the frequency spectra of the real and imaginary parts of the complex permittivity and the tangent losses for two thermosetting composites composed of lossy waste materials.

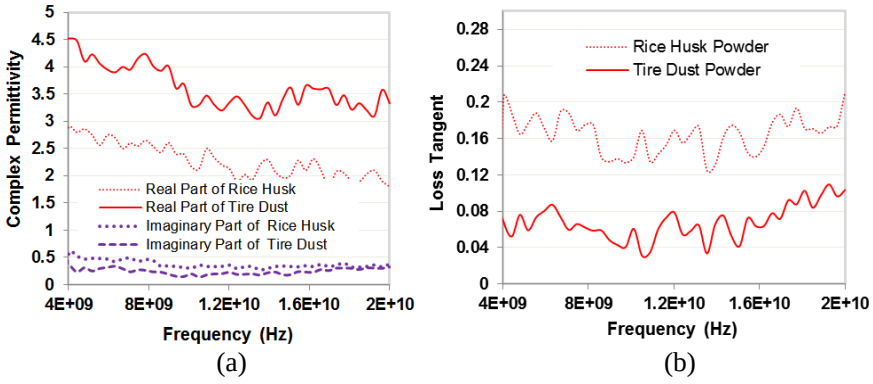

Figure 2. Behavior of the dielectric properties of two thermoset composites composed of two waste materials. (a) Complex permittivity. (b) Spectrum of loss tangent.

These composite samples were fabricated manually at room temperature by mixing unsaturated polyester resin (UPR) separately with the powders of rice husks from a crop residue and rubber from discarded automobile tires. The rice husk-based composite had lower ε'_r values than the sample that was composed of rubber from scrap tires. The ε'_r values for the rice husk-based composite were between 1.8 and 2.9, while for the composite composed of rubber had values between 3.0 and 4.5. These values indicate that the incident wave will experience less discontinuity in the permittivity, and hence impedance, while propagating from air to the rice-husk composite.

Values of tangent loss ($\varepsilon''_r/\varepsilon'_r$), which is better known as dissipation factor, for the rice-husk composite were between 0.1 and 0.2, while these values were less than 0.1 for the rubber-based composite. This indicates that the dissipation of electromagnetic energy will be greater in the rice husk-based composite and that a thinner material will be required to attenuate the wave.

3.2. Wave Propagation and Attenuation

Figures 3(a) and (b) show the attenuation constant ($\alpha(\omega)$) and depth of penetration ($d(\omega)_p$) for two composites, one composed of rice husks and one composed of rubber from scrap tires, respectively.

It is apparent that the value of $\alpha(\omega)$ for both of the composites increased as the frequency increased throughout the spectrum. In addition, it can be seen that $\alpha(\omega)_{rice} > \alpha(\omega)_{rubber}$, which is due to

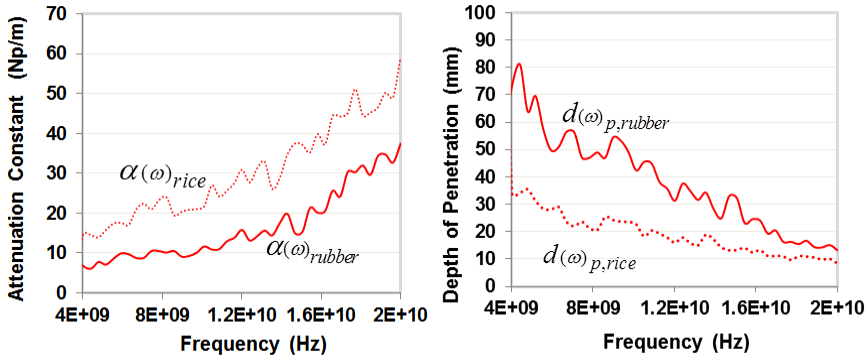

Figure 3. Characteristics of two waste materials as a function of frequency based on the measured dielectric properties. (a) Attenuation constant. (b) Depth of penetration.

the fact that $\varepsilon''(\omega)_{rice} > \varepsilon''(\omega)_{rubber}$, where α and ε_r'' are related by the following expression (for $\mu = 1 - j0$) [25].

$$\alpha(\omega) = \frac{\omega}{\sqrt{2}c}\sqrt{\sqrt{(\varepsilon_r'^2 + \varepsilon_r''^2)} - \varepsilon_r'} \tag{1}$$

Figure 3(b) shows that the values of depth of penetration $d(\omega)_{p,rice} < d(\omega)_{p,rubber}$ and for the rice-husk based composite were between 10 and 39 mm, while the values for the rubber-based composite were in the range of 15 to 80 mm.

Normalized characteristic impedance $z = 120\pi(\varepsilon_r' - j\varepsilon_r'')^{-0.5}$ and the power reflected from the rice husk-based composite (RHC) and the rubber-tire composite (RTC) relative to free space are shown in the Figure 4(a). It can be observed that the reflected power from both of the dielectric composites decreased as frequency increased. This can be attributed to the mismatch ($\varepsilon(\omega) \neq \varepsilon_0$) in the values of the permittivity.

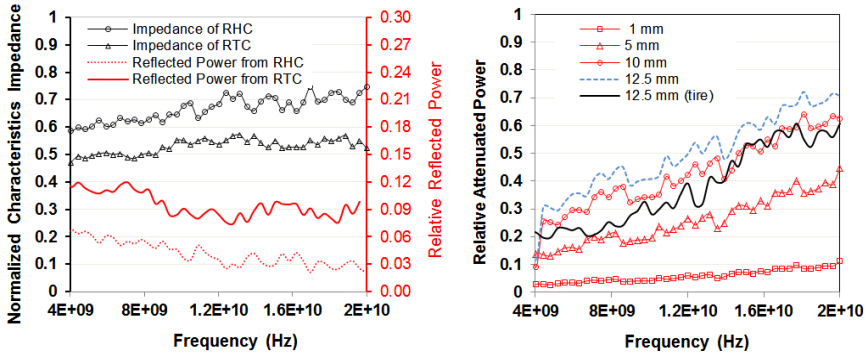

Figure 4. (a) Magnitude of normalized characteristic impedance and reflected power from the RHC and RTC relative to free space. (b) Frequency spectrum of attenuated power relative to free space for different thicknesses of RHC.

In addition, the values of reflected power are in the range of 3% to 6% for the RHC, while they are in the range of 9% to 12% of the power of the incident wave for RTC. The remainder of the signal's power was further decreased exponentially ($e^{-\alpha d}$) while the signal was traversing the thickness d of the medium that was characterized by the spatial attenuation coefficient α. The net attenuated power ($1 - e^{-2\alpha d}$) relative to the free space, which was absorbed within the thickness d, is plotted in Figure 4(b). It is obvious that the attenuation of the

signal increased as the thickness of the RHC increased. However, for the same thickness (12.5 mm) RHC offered 10% more attenuation to the signal as compared to the RTC.

4. RESULTS AND DISCUSSION

4.1. Simulated Results

We performed a parametric study, and the thickness of the clad material (t) was chosen as the parameter to be varied, such as $0 < t < 25$ mm, in six 5-mm steps. Simulations were performed for two cases, i.e., 1) RHC was used as the outer pyramidal clad and RTC was used as the inner pyramidal core and 2) the positions of the RHC and the RTC were reversed. The overall dimensions of the absorber that was simulated were as follows. The heights of the pyramidal and square base parts were 100 mm and 20 mm, respectively, while both the width and length of the base were 50 mm. The distance between the excitation port and the pyramidal absorbers was 300 mm.

4.1.1. One-port Results with Perfect Electric Conductor (PEC) Backed

Figure 5(a) shows the effect of the RHC clad on the reflectivity profiles of a pyramidal absorber that had an RTC inner pyramidal core, whereas the effects of the RTC clad on the RHC inner pyramidal core are shown in Figure 5(b).

It is clear from Figure 5(a) that better reflectivity profiles were obtained as the RHC clad thickness was increased for all values ($t > 0$) of clad thicknesses. The threshold thickness of the RHC clad was found to be 5 mm for which better (lower) than −15 dB results (in the 4 to 20 GHz range) were obtained. In addition, at 6 GHz, less than −20 dB resulted for 5 mm of RHC clad thickness, which are the minimum requirement for commercial anechoic chambers according to CISPR11. The threshold (minimum) thickness of RHC clad for better (lower) than −20 dB reflectivity was found to be 10 mm in the frequency range of 4 to 20 GHz, whereas, lower than −30 dB started at 8 GHz. Minimum clad thickness was found to be 15 mm for which lower than −30 dB reflectivity performance started at 6 GHz and reached a level lower than −40 dB at 9 GHz. Moreover, it can be seen that reflectivity performance improved as the thickness of RHC clad increased, and the best results (−25 dB) were obtained at the lowest frequency (4 GHz) for the case of an RHC clad thickness of 25 mm. However, in this case the entire absorber was composed of RHC (with no RTC inner core).

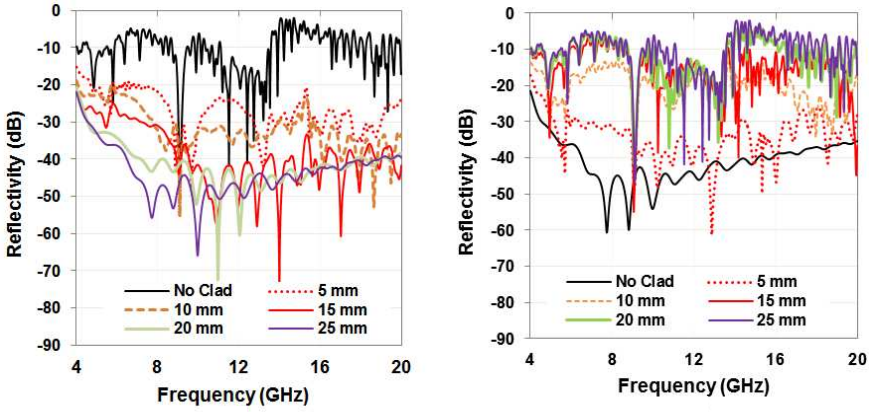

Figure 5. One-port reflectivity performance of a pyramidal absorber with different clad thicknesses. (a) Low ε_r' and high ε_r'' RHC clad-based absorber. (b) High ε_r' and low ε_r'' RTC clad-based absorber.

This is outside the scope of the current discussion and is presented only for comparison.

Analysis of the results shown in the Figure 5(b) depicts that the performance of the absorber decreased with increases in the thickness of the RTC clad on the inner RHC pyramidal core. Reflectivity curves could not attain the level of -20 dB for the thicknesses of RTC clad greater than 10 mm, and the worst performance was observed in the case of $t = 25$ mm, which corresponds to the full RTC pyramidal absorber. Decrease in performance as the RTC clad thickness increased was attributed to the lower attenuation (dissipation) and higher reflection values of the RTC. In order to confirm this, we performed two-port simulations, and the results are discussed in the following section.

4.1.2. Two-port Results without PEC Back Plate

Figure 6(a) and Figure 7(a) shows that with increase in the clad thickness, better performance, i.e., lower values of reflection loss, was observed for the case of RHC absorber, while, conversely, the performance of the RTC absorber decreased.

Further, Figure 6(b) shows that, in the case of the RHC-clad absorber, the amplitude of the transmitted signal decreased as the thickness of the clad increased. This transmission loss was due totally to the absorption of the signal within the absorber because absorption

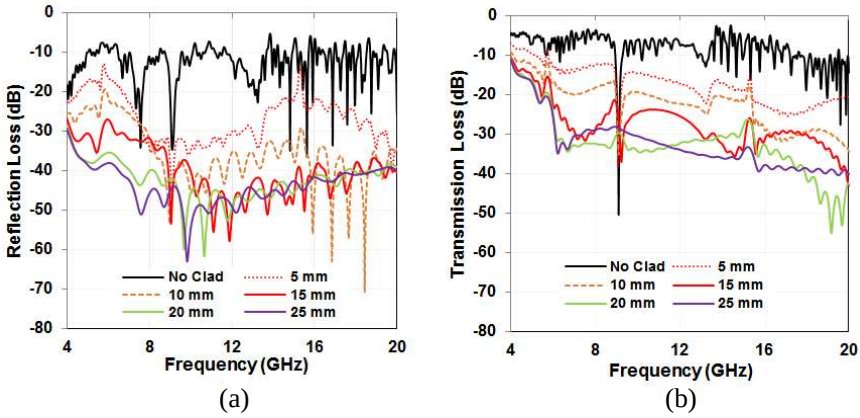

Figure 6. Two-port simulated results for different thicknesses of RHC clad. (a) Reflection loss. (b) Transmission loss.

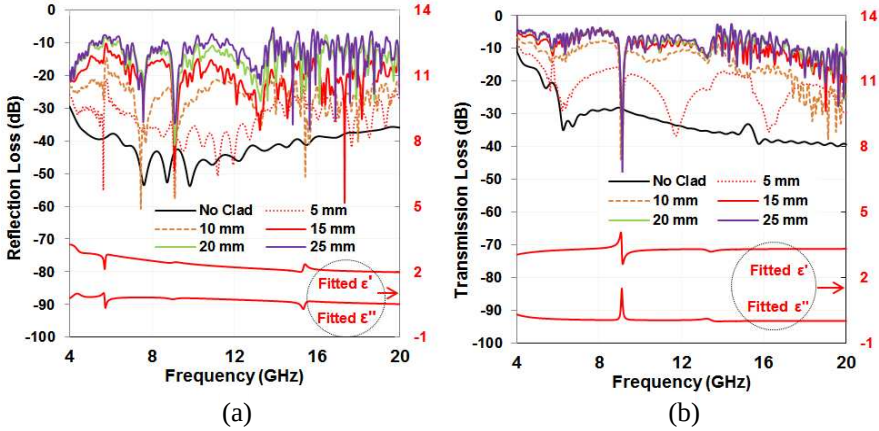

Figure 7. Two-port simulated results for different thicknesses of RHT clad. (a) Reflection loss along with the nth-order-fitted dielectric properties of RHC material. (b) Transmission loss along with the nth-order-fitted dielectric properties of RTC material.

depends upon reflection and the transmission loss. A perfect absorber must have better (lower) reflection and transmission losses.

In all of the results that we have presented, some peaks were observed, and most of them were due to inhomogeneities in the materials and to the capacitive behavior of systems composed of lossy

fillers and polymer resin. Figure 7(a) is a plot of the nth order-fitted data (by CST software) of the dielectric properties of the RHC material, while the fitted data for RTC are shown in Figure 7(b), along with the transmission loss spectrum. It can be seen that at 9 GHz, the value of loss factor ε_r'' increased, while the value of ε_r' decreased and all of the curves for the RTC clad absorber had a deep null at this frequency. Whereas, in the case of the RHC material, the values of ε_r' and ε_r'' both decreased at 5.75 GHz (Figure 7(a)), and, as a consequence of this decrease, an increase (worse performance) in the reflection loss and transmission loss values were observed at this frequency.

4.1.3. Impulse Response of Absorbers

Figure 8 shows the impulse response of two cladded pyramidal absorbers. The first reflection occurred simultaneously from the tips of both absorbers at 1.35 ns.

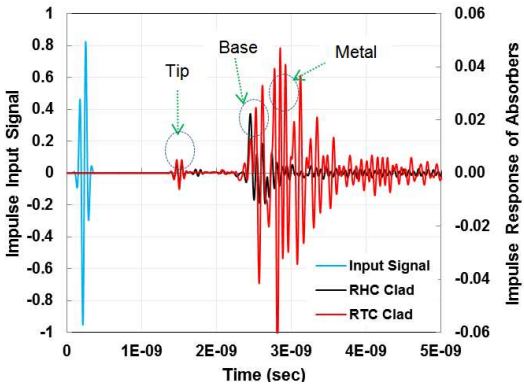

Figure 8. Impulse response of RHC clad and RTC clad absorbers showing a brief input signal and reflections from tips, base, and metal back PEC.

The amplitude of the tip-reflected signal from the RHC clad absorber was smaller than that of the RTC clad absorber because the RHC clad absorber had low permittivity and better impedance matching at its tip. Another small, reflected peak was observed at 1.60 ns only for RHC clad absorber, and it was due to the presence of the high-permittivity, inner pyramidal core of the RTC absorber.

Times of arrival of the signals that were reflected from the base and PEC plate were found to be 2.34 ns and 2.60 ns, respectively, in the case of the RHC clad absorber. However, these reflected signals had smaller

amplitudes than those of the RTC clad absorber, and this can be explained on the basis of impedance analysis as follows. For the RHC clad absorber, the inner pyramidal core (RTC) had low impedance and was backed by a low impedance PEC. In the case of the RTC clad absorber, the inner pyramidal core (RHC) had high impedance, hence large reflections occurred due to the impedance mismatch. This time-domain analysis also validated our conclusion that the RHC-clad pyramidal absorber with an RTC inner core will have less reflection (better anechoic performance).

4.2. Measured Results

The performance of an anechoic chamber depends on its size and shape [26], but the performance of an absorber can be determined by measuring its reflectivity, $R = 20 \log |\Gamma|$, in dB. Here, $\Gamma = E_r/E_i$ is known as the reflection coefficient and is the comparison of the amplitudes of the reflected electric field (E_r) and the incident electric field (E_i). For better absorption, smaller values of reflectivity over a broad frequency range are desired. In this study, we used the free-space reflectivity measurement method (similar to the naval research laboratory (NRL) arch method) using two-horn antennas along with a programmable network analyzer (PNA). This is a contactless, non-destructive, and easy-to-arrange method that provides a flexible measurement setup under various conditions. An absorber fabricated in an array of 3×3 pyramids was placed in far field region of the horn antennas, and both antennas were well isolated by using absorbing material. Measured and simulated reflectivity profiles as a function of frequency for normal incidence with and without the square base part of the pyramidal absorber are shown in Figures 9(a) and (b), respectively.

The simulated and measured results are in good agreement, and, in addition, performance better (lower) than −20 dB began at 6.5 GHz for the absorber that had no base part. Reflectivity performance lower than −30 dB began at 7 GHz, and, with the integration of the base and pyramidal parts in the absorber, attained the value of −35 dB at 8 GHz. The RHC clad absorber with a 20-mm base part showed the best performance in the frequency range of 8 to 10 GHz, where some of the peaks attained the value of −48 dB.

In [14], it was shown that the performance of an absorber based on a mixture of tire dust and rice husks was between −23 dB and −27 dB in the frequency range of 7 to 13 GHz. Figure 9(b) shows that the RHC clad absorber that we designed and tested had an overall performance that was better than −30 dB in the range of 7 to 13 GHz, and, after 8 GHz, the results were between −35 and −48 dB.

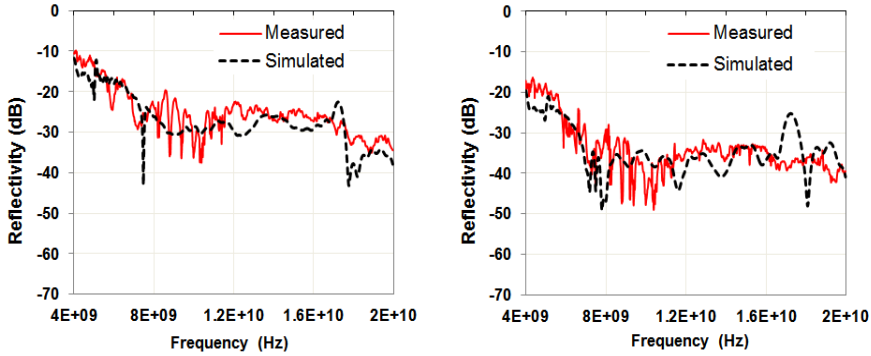

Figure 9. Reflectivity performance of RHC-cladded, RTC pyramidal absorber in an array of 3×3 for normal incidence. (a) Results of absorber without base part. (b) Results of absorber with a 20-mm base part.

5. CONCLUSIONS

Based on the results of this study, we conclude that a low-permittivity, rice-husk clad can be used to improve the anechoic performance of a pyramidal absorber that is composed of relatively higher permittivity rubber from scrap tires. In addition, this approach offers an extra degree of freedom to optimize the anechoic performance of any absorber that does not satisfy the minimum requirements of either -10 dB or -20 dB. Millions of tires are being manufactured and utilized in the automobile industry; however, after their life span, they merely contribute to our burgeoning landfill waste. Likewise, millions of tons of rice husks are dumped or even burned, resulting in detrimental impacts on the environment. The main contribution of studies such as ours is that two waste materials can be used in a low-cost, value-added product, i.e., microwave absorbers.

REFERENCES

1. MIL-STD-461F, "Requirements for the control of electromagnetic interference characteristics of subsystems and equipment," Department of Defense Interface Standard, USA, 2007.
2. Tong, X. C., *Advanced Materials and Design for Electromagnetic Interference Shielding*, CRC Press, Taylor & Francis Group, Broken Sound Parkway NW, Suite 300, Boca Raton, 2009.

3. Glaser, J. I., "Stealthy antennas minimizing the radar cross section of an essential communication system component," *The WSTIAC Quarterly*, Vol. 8, No. 2, 2008.
4. Ford, K. L. and B. Chambers, "Improvement in the low frequency performance of geometric transition radar absorbers using square loop impedance layers," *IEEE Transactions on Antennas and Propagation*, Vol. 56, No. 1, 133–141, Jan. 2008.
5. Ford, K. L., D. Holtby, and B. Chambers, "Pyramidal absorbers loaded with resistive FSS," *IEEE Antennas and Propagation Society International Symposium*, 4553–4556, 2007.
6. Nornikman, H., F. Malek, P. J. Soh, A. A. H. Azremi, F. H. Wee, and A. Hasnain, "Parametric studies of the pyramidal microwave absorber using rice husk," *Progress In Electromagnetics Research*, Vol. 104, 145–166, 2010.
7. Nornikman, H., P. J. Soh, A. A. H. Azremi, M. R. N. Husna, and O. S. Liam, " Parametric study of pyramidal microwave absorber design," *International Symposium on Antennas and Propagation (ISAP 2008)*, Taipei, Taiwan, Oct. 27–30, 2008.
8. Nornikman, H., P. J. Soh, and A. A. H. Azremi, "Modeling simulation stage of pyramidal and wedge absorber microwave absorber design," *4th International Conference on Electromagnetic Near Field Characterization and Imaging (ICONIC' 09)*, 238–242, Taipei, Taiwan, Jun. 24–26, 2009.
9. Nornikman, H., P. J. Soh, and A. A. H. Azremi, "Performance simulation of pyramidal and wedge microwave absorbers," *3rd Asian Modeling Symposium (AMS 2009)*, 649–654, Bandung, Indonesia, May 25–26, 2009.
10. Nornikman, H., F. Malek, P. J. Soh, and A. A. H. Azremi, "Reflection loss performance of hexagonal base pyramid microwave absorber using different agricultural waste material," *2010 Loughborough Antennas & Propagation Conference*, 313–316, Loughborough, UK, Nov. 8–9, 2010.
11. Nornikman, H., P. J. Soh, F. Malek, A. A. H. Azremi, F. H. Wee, and R. B. Ahmad, "Microwave wedge absorber design using rice husk — An evaluation on placement variation," *2010 Asia-Pacific International Symposium on Electromagnetic Compatibility*, 916–919, Beijing, China, Apr. 12–16, 2010.
12. Nornikman, H., F. Malek, P. J. Soh, A. A. H. Azremi, F. H. Wee, and A. Hasnain, "Setup and results of pyramidal microwave absorbers using rice husks," *Progress In Electromagnetics Research*, Vol. 111, 141–161, 2011.
13. Nornikman, H., P. J. Soh, A. A. H. Azremi, F. H. Wee,

and M. F. Malek "Investigation of an agricultural waste as an alternative material for microwave absorbers," *PIERS Online*, Vol. 5, No. 6, 506–510, 2009.

14. Malek, F., E. M. Cheng, O. Nadiah, H. Nornikman, M. Ahmed, M. Z. A. A. Aziz, A. R. Othman, P. J. Soh, A. A. H. Azremi, A. Hasnain, and M. N. Taib, "Rubber tire dust-rice husk pyramidal microwave absorber," *Progress In Electromagnetics Research*, Vol. 117, 449–477, 2011.
15. Cheng, E. M., F. Malek, M. Ahmed, K. Y. You, K. Y. Lee, and H. Nornikman, "The use of dielectric mixture equations to analyze the dielectric properties of a mixture of rubber tire dust and rice husks in a microwave absorber," *Progress In Electromagnetics Research*, Vol. 129, 559–578, 2012.
16. Malek, F., H. Nornikman, and O. Nadiah "Pyramidal microwave absorber design of waste material using rice husk and rubber tire dust," *Journal of Telecommunication, Electronic and Computer Engineering*, Vol. 4, No. 1, Jan.–Jun. 2012.
17. Wan Ab Karim Ghani, W. A., M. S. F. Abdullah, K. A. Matori, A. B. Alias, and G. da Silva, "Physical and thermochemical characterization of Malaysian biomass ashes," *Journal — The Institution of Engineers*, Vol. 71, No. 3, Malaysia, Sep. 2010.
18. Wang, M. J., Y. F. Huang, P. T. Chiueh, W. H. Kuan, and S. L. Lo, "Microwave-induced torrefaction of rice husk and sugarcane residues," *Energy*, Vol. 37, 177–184, 2012.
19. Bantsis, G., S. Mavridou, C. Sikalidis, M. Betsiou, N. Oikonomou, and T. Yioultsis, "Comparison of low cost shielding-absorbing cement paste building materials in X-band frequency range using a variety of wastes," *Ceramics International*, Vol. 38, 3683–3692, 2012.
20. Aylón, E., A. Fernández-Colino, R. Murillo, G. Grasa, M. V. Navarro, T. García, and A. M. Mastral, "Waste tyre pyrolysis: Modeling of a moving bed reactor," *Waste Management*, Vol. 30, 2530–2536, 2010.
21. Hasar, U. C., "An accurate complex permittivity method for thin dielectric materials," *Progress In Electromagnetics Research*, Vol. 91, 123–138, 2009.
22. Li, E., Z. P. Nie, G. Guo, Q. Zhang, Z. Li, and F. He, "Broadband measurement of dielectric properties of low-loss materials at high temperature using circular cavity method," *Progress In Electromagnetics Research*, Vol. 92, 103–120, 2009.
23. Hasar, U. C., G. Akkaya, M. Aktan, C. Gozu, and A. C. Aydin, "Water-to-cement ratio prediction using anns from non-

destructive and contactless microwave measurements," *Progress In Electromagnetics Research*, Vol. 94, 311–325, 2009.

24. Paez, E., M. A. Azpurua, C. Tremola, and R. C. Callarotti, "Uncertainty estimation in complex permittivity measurements by shielded dielectric resonator technique using the Monte Carlo method,," *Progress In Electromagnetics Research B*, Vol. 41, 101–119, 2012.
25. Qin, F. and C. Brosseau, "A review and analysis of microwave absorption in polymer composites filled with carbonaceous particles," *J. Appl. Phys.*, Vol. 111, 061301, 2012.
26. Holloway, C. L., R. R. DeLyser, R. F. German, P. McKenna, and M. Kanda "Comparison of electromagnetic absorber used in anechoic and semi-anechoic chambers for emissions and immunity testing of digital devices," *IEEE Trans. Electromag. Compat.*, Vol. 39, No. 1, 33–47, Feb. 1997.